How to cite: Angew. Chem. Int. Ed. 2024, e202403834
doi.org/10.1002/anie.202403834

Polymer Chemistry Hot Paper

Nanogels with Metal-Organic Cages as Functional Crosslinks

*Chaolei Hu and Kay Severin**

Abstract: A dinuclear metal-organic cage with four acrylate side chains was prepared by self-assembly. Precipitation polymerization of the cage with N-isopropylacrylamide yielded a thermoresponsive nanogel. The host properties of the cage were retained within the gel matrix, endowing the nanogel with the capability to serve as a sorbent for chloride ions in water. Moreover, a heteroleptic cage with the drug abiraterone as co-ligand was integrated into a nanogel. The addition of chloride ions induced a structural rearrangement of the metal-ligand assembly, resulting in the gradual release of abiraterone.

Introduction

Micro- and nanogels differ from normal macroscopic gels in that the size of the gel network is in the range of micrometers or below.[1] They are soft colloids when swollen by the solvent, and they can display stimuli-responsive behavior.[1,2] Micro- and nanogels have been examined for diverse applications, including drug delivery,[3] chemosensing,[4] catalysis,[4,5] and the fabrication of thermoresponsive materials.[6]

Tailoring the properties of micro- and nanogels is achievable through the integration of functional subunits (e.g. bioactive molecules, metal nanoparticles, or photochromic molecules).[1–6] So far, there are limited reports about the use of coordination complexes as responsive components in micro/nanogels. Sanson, Perrin, and coworkers have prepared microgels containing $[Fe^{II}(terpyridine)_2]^{2+}$ complexes as crosslinks.[7] Chemically-triggered destruction of the microgels was achieved by oxidation of the Fe^{II} complexes. Metal terpyridine complexes were also used for the reversible assembly of microgel particles.[8]

We wanted to explore if metal-organic cages (MOCs) could be used as crosslinks in micro- or nanogels. MOCs are polynuclear complexes with defined cavities.[9] Typically, MOCs are obtained by self-assembly using polytopic ligands and metal complexes (or ions) with two or more available coordination sites.[9] The interior of MOCs can be used for binding ions, gases, or larger molecules.[10] Furthermore, MOCs have been used as nanoreactors for chemical transformation.[11] The dynamic nature of metal-ligand bonds confers structural malleability upon MOCs. Consequently, these cages can be disassembled or rearranged in response to specific external stimuli, such as light exposure, chemicals, or alterations in pH.[12]

Several research groups have studied the incorporation of MOCs into soft materials such as organo- or hydrogels.[13] To the best of our knowledge, there are no reports about the integration of MOCs into micro- or nanogels. Below, we show that palladium-organic cages with acrylamide side chains can be incorporated in N-isopropylacrylamide-based nanogels by precipitation polymerization. Due to the presence of MOC crosslinks, the resulting nanogels can be used as specific sorbents for chloride ions, and for the stimuli-responsive release of the drug abiraterone.

Results and Discussion

For our investigations, we opted to use a dinuclear Pd^{II} complex with four bridging 1,3-di(pyridin-3-yl)benzene ligands as the core cage structure. This particular MOC exhibits an inherent capacity for structural rearrangements.[14] Moreover, it displays a high affinity for small anions, notably chloride.[15]

Micro- and nanogels are conventionally prepared by radical polymerization of suited monomers.[16] Hence, we had to functionalize the dipyridyl ligand with a polymerizable side chain. Ligand **L1** was synthesized by coupling of acryloyl chloride to a 1,3-di(pyridin-3-yl)benzene ligand containing a tetraethyleneglycol side chain at the central phenylene group. The latter was prepared in three steps from readily available compounds (for details, see the Supporting Information). The presence of the acrylate side chain did not interfere with cage formation: when **L1** (2 eq.) was heated with $Pd(NO_3)_2$ in CD_3CN to 80 °C for two hours, the clean formation of the MOC $[Pd_2(\mathbf{L1})_4(NO_3)](NO_3)_3$ was observed, as evidenced by NMR spectroscopy and mass spectrometry (Scheme 1, Figure 1).

Upon coordination of **L1** to Pd^{2+}, the ^1H NMR signals of the aromatic C-H protons were shifted towards lower field (Figure 1b). The largest shifts were observed for the protons 'a' and 'f'. These protons point to the interior of the cage, and they are likely involved in C–H···O hydrogen bonds to a nitrate anion, which is bound in the cavity of the cage.[15]

[*] Dr. C. Hu, Prof. K. Severin
Institut des Sciences et Ingénierie Chimiques, Ecole Polytechnique Fédérale de Lausanne (EPFL), 1015, Lausanne, Switzerland
E-mail: kay.severin@epfl.ch

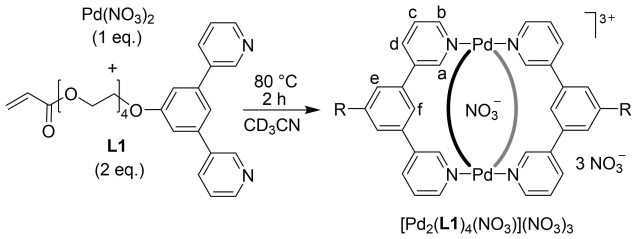

Scheme 1. Synthesis of cage $[Pd_2(\mathbf{L1})_4(NO_3)](NO_3)_3$.

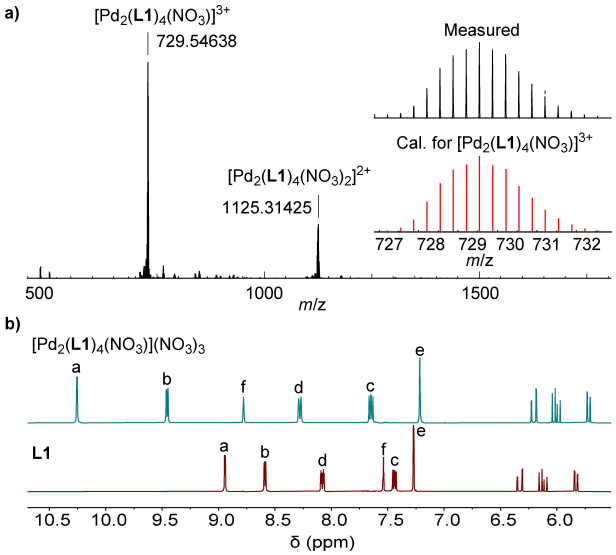

Figure 1. Characterization of $[Pd_2(\mathbf{L1})_4(NO_3)](NO_3)_3$ by high-resolution ESI mass spectrometry (**a**) and ^{1}H NMR spectroscopy (400 MHz, CD_3CN, region of aromatic/olefinic protons) (**b**). Part of the ^{1}H NMR spectrum of ligand **L1** is given as a reference.

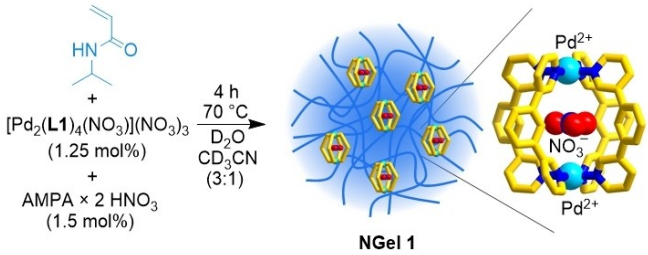

Scheme 2. Synthesis of **NGel 1** by precipitation polymerization of a mixture of N-isopropylacrylamide and $[Pd_2(\mathbf{L1})_4(NO_3)](NO_3)_3$ with 2,2'-azobis(2-amidinopropane) (AMPA) as initiator.

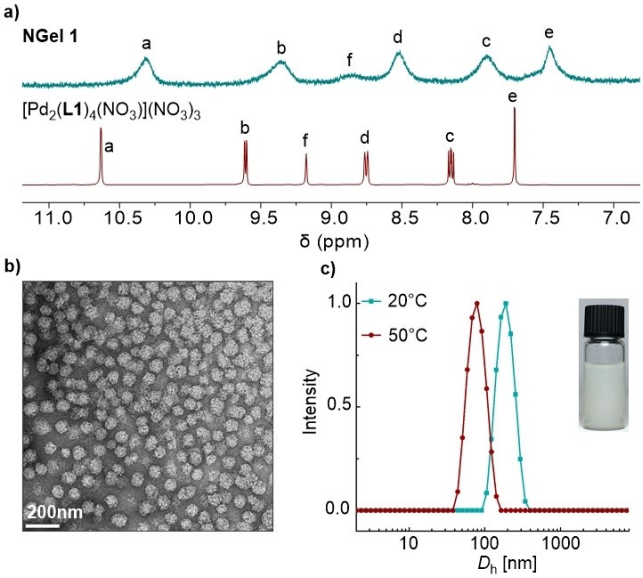

Figure 2. (**a**) Part of the ^{1}H NMR spectrum (400 MHz, D_2O/CD_3CN, 3:1; 283 K) of **NGel 1** along with the spectrum of $[Pd_2(\mathbf{L1})_4(NO_3)](NO_3)_3$ (D_2O/CD_3CN, 3:1) as a reference. (**b**) TEM image of **NGel 1** (stained with uranyl acetate, 200 kV, scale bar 200 nm). (**c**) Size distribution of **NGel 1** in water at 20 °C and 50 °C, respectively, as determined by DLS. The inset shows a picture of a dispersion of **NGel 1** in water at room temperature.

Subsequently, we investigated if $[Pd_2(\mathbf{L1})_4(NO_3)](NO_3)_3$ could be incorporated into micro/nanogels. The co-polymerization of the MOC with N-isopropylacrylamide (NIPAM), a commonly used monomer,[16] was carried out using the radical initiator 2,2'-azobis(2-amidinopropane) (AMPA). AMPA is supplied as a hydrochloride salt. The chloride anion in the azo initiator could lead to a $NO_3^- \rightarrow Cl^-$ exchange in the cage cavity. To avoid such an exchange, we first converted AMPA × 2 HCl into AMPA × 2 HNO_3 by reaction with $AgNO_3$ (for details, see the Supporting Information). Subsequent to this modification, the co-polymerization was conducted at 70 °C in a mixture of D_2O and CD_3CN (3:1) using 1.25 mol % of $[Pd_2(\mathbf{L1})_4(NO_3)](NO_3)_3$ with respect to NIPAM (Scheme 2).

Within 30 minutes, the mixture became turbid, indicating the formation of a colloidal dispersion. After 4 hours, the system was allowed to cool to room temperature, and an initial analysis of the product, **NGel 1**, was performed by ^{1}H NMR spectroscopy. As anticipated, we observed broad signals. The multiplicity and the chemical shifts were similar to what was observed for $[Pd_2(\mathbf{L1})_4(NO_3)](NO_3)_3$ (Figure 2a). This result suggested that the structure of the metal-ligand assembly had not been compromised by the radical polymerization. By integrating selected ^{1}H NMR signals, we were able to deduce that **NGel 1** contains approximately 0.8 mol % of cage crosslinks (see the Supporting Information, Figure S13 and Table S1).

Following the initial NMR analysis, **NGel 1** was purified by dialysis against deionized water for one week. The resulting colloid was then characterized by TEM and DLS measurements. TEM imaging unveiled uniform spherical particles with a mean diameter of approximately 80 nm (Figure 2b and the Supporting Information, Figure S14). The average hydrodynamic diameter (D) of **NGel 1** in water at 20 °C was found to be 180 nm (Figure 2c and the Supporting Information, Table S2). This value is larger than what was determined by TEM because the nanogel is swollen in water. The particles exhibited a narrow size distribution, reflected by a low PDI of 0.04 (see the Supporting Information, Table S2).

NGel 1 was found to be thermoresponsive: DLS measurements at 50 °C gave a hydrodynamic diameter of 75 nm, with a deswelling value of 0.071 (see the Supporting Information, Table S2). The volume phase transition temperature (VPTT) of **NGel 1** was 36 °C, as determined by temperature-dependent DLS measurements (see the Supporting Information, Figure S15 and Table S2).

In earlier work, we had shown that a dinuclear MOC with bridging 1,3-di(pyridin-3-yl)benzene ligands represents a highly potent receptor for chloride, with an affinity in water in the micromolar concentration range.[15] Since **NGel 1** contains closely related MOCs, it was expected to act as a sorbent for chloride ions.

The exchange of nitrate for chloride in cages of type $[Pd_2(\mathbf{L1})_4(NO_3)](NO_3)_3$ was expected to result in a large downfield shift of the ^{1}H NMR signal of the aromatic NC–H protons 'a'.[15] Given this substantial change, we anticipated that chloride ion binding by **NGel 1** could be monitored by NMR spectroscopy, despite the inherently broad NMR signals of **NGel 1**. Indeed, when aliquots of a solution of NaCl in D_2O were added to a dispersion of freshly prepared **NGel 1** in D_2O/CD_3CN (3:1), a new ^{1}H NMR signal at approximately 10.7 ppm could be observed (Figure 3). This signal indicates the presence of MOC crosslinks with bound chloride. The anion exchange could be reversed by the addition of $AgNO_3$ (for details, see the Supporting Information, Section 3.1).

To demonstrate that **NGel 1** is able to act as a chloride sorbent in pure water, we added NaCl to a dispersion of **NGel 1** in D_2O. The chloride concentration in the mixture, set at 0.50 mM, corresponded to the anticipated concentration of MOC crosslinks in the dispersion. Following a 2-hour incubation period, the nanogel was isolated via centrifugation, and the chloride content in the supernatant was quantified utilizing a soluble MOC receptor with a known affinity for Cl^- (for details, see the Supporting Information, Section 3.2). The analysis revealed a reduction in chloride content from 0.50 mM to 0.21 mM, indicating that a significant portion of the MOCs within **NGel 1** possess chloride binding properties akin to their soluble counterparts.[17] These findings provide compelling evidence of the chloride-binding capacity of **NGel 1**, reinforcing its potential as an effective sorbent material.

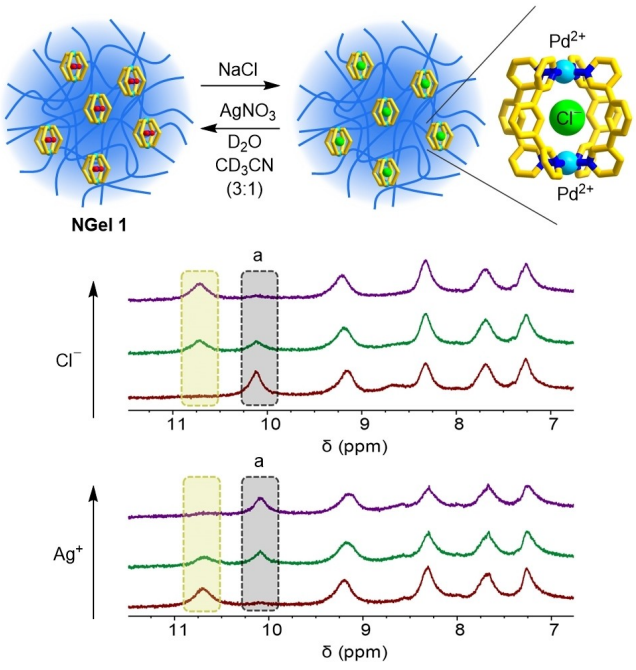

Figure 3. Chloride ion binding by **NGel 1** and subsequent chloride ion removal with $AgNO_3$ as evidenced by ^{1}H NMR spectroscopy (400 MHz, D_2O/CD_3CN, 3:1; 283 K).

As mentioned above, Pd^{II} cages featuring bridging 1,3-di(pyridine-3-yl)benzene ligands exhibit a propensity for structural rearrangements. Notably, heteroleptic cages incorporating two distinct ligands frequently display enhanced stability compared to their homoleptic counterparts.[14] We were interested if ligand exchange reactions could be realized within a nanogel. In particular, we wanted to examine if a structural rearrangement could be used to liberate a pharmacologically relevant compound.

The anticancer drug abiraterone (**Abi**)[18] was selected as the bioactive compound for this study. This drug features a 3-pyridyl group, which was expected to enable its coordination to Pd^{2+}. When a mixture of **L1** (3 eq.), abiraterone (2 eq.), and $[Pd(CH_3CN)_4](BF_4)_4$ (2 eq.) in CD_3CN was heated to 80 °C for 12 hours, the formation of a defined heteroleptic complex was observed. According to NMR and MS data (Figure S20 and S22), this complex had the formula $[Pd_2(\mathbf{L1})_3(\mathbf{Abi})_2](BF_4)_4$ (Scheme 3a). The high stability of the heteroleptic complex was substantiated by the following experiment: when one equivalent of ligand **L1** was added to a solution of $[Pd_2(\mathbf{L1})_3(\mathbf{Abi})_2](BF_4)_4$ in D_2O/CD_3CN (3:1), no reaction was observed, even after heating the mixture for 2 hours at 80 °C (see the Supporting Information, Figure S36). However, a rearrangement into $[Pd_2(\mathbf{L1})_4(Cl)](BF_4)_3$ and 'free' **Abi** could be induced by the addition of one equivalent of NaCl (see the Supporting Information, Figure S37).

The integration of complex $[Pd_2(\mathbf{L1})_3(\mathbf{Abi})_2](BF_4)_4$ into a nanogel was achieved by co-polymerization with NIPAM using the initiator AMPA × 2 HBF_4. The co-polymerization was carried out at 70 °C in a mixture of D_2O and CD_3CN (3:1) using 2.5 mol % of $[Pd_2(\mathbf{L1})_3(\mathbf{Abi})_2](BF_4)_4$ and 2.5 mol % of **L1** with respect to NIPAM (Scheme 3b). An initial analysis of the product **NGel 2** by ^{1}H NMR spectroscopy yielded limited information. The heteroleptic crosslinks in **NGel 2** gave rise to a high signal multiplicity, and peak broadening due to colloid formation compromised an interpretation.

NGel 2 was purified by dialysis against mixed solvents of acetone and deionized water (1:1) for 5 days and deionized water for 5 days. The resulting colloid was then characterized by TEM and DLS measurements. The TEM image revealed spherical particles with a mean diameter of approximately 108 nm (see the Supporting Information, Figure S27). While this value is similar to what was found for **NGel 1** (80 nm), the size of the **NGel 2** particles was less uniform. The average hydrodynamic diameter of **NGel 2** in

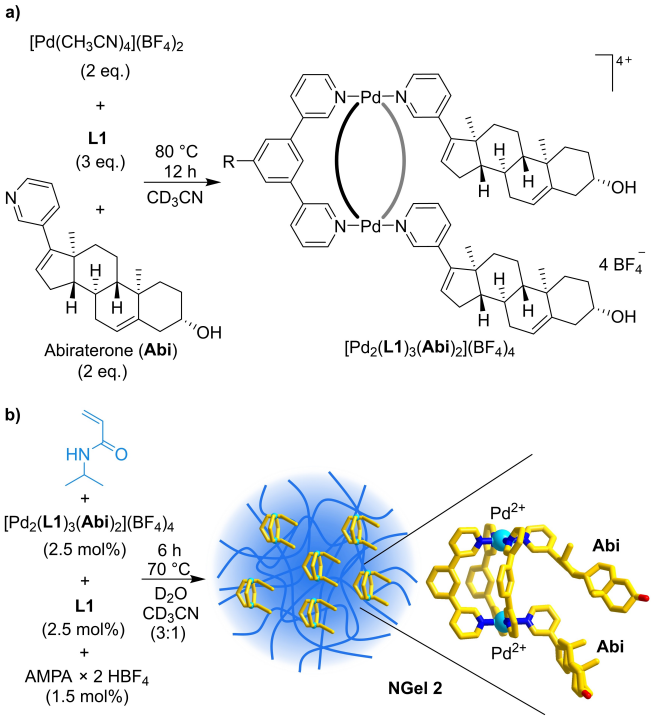

Scheme 3. (**a**) Synthesis of the heteroleptic complex $[Pd_2(\mathbf{L1})_3(\mathbf{Abi})_2](BF_4)_4$. (**b**) Synthesis of **NGel 2** by precipitation polymerization of a mixture of N-isopropylacrylamide, $[Pd_2(\mathbf{L1})_3(\mathbf{Abi})_2](BF_4)_4$ and **L1** with 2,2'-azobis(2-amidinopropane) (AMPA) as initiator.

water at 20 °C was 190 nm (see the Supporting Information, Figure S28, Table S3). Similar to **NGel 1, NGel 2** was found to be thermoresponsive: DLS measurements at 50 °C gave a hydrodynamic diameter of 75 nm, with a deswelling value of 0.414 (see the Supporting Information, Table S3). The higher deswelling value of **NGel 2** when compared to **NGel 1** indicates that the particles are more rigid. The volume phase transition temperature (VPTT) of **NGel 2** was 39 °C, as determined by temperature-dependent DLS measurements (see the Supporting Information, Figure S29 and Table S3). The higher VPTT of **NGel 2** compared to **NGel 1** can be attributed to the increased charge of **NGel 2** (see the Supporting Information, Figure S30).

Next, we examined if a chloride-induced rearrangement of the Pd-based crosslinks could be achieved within the nanogel matrix. By co-polymerizing the heteroleptic cage with one equivalent of **L1**, **NGel 2** contained a surplus of bipyridyl ligands, allowing for the formation of a homoleptic, chloride-bound cage. NMR measurements with freshly prepared **NGel 2** substantiated the feasibility of such an anion-induced rearrangement. Upon the addition of one equivalent of NaCl to a dispersion of **NGel 2** in D_2O/CD_3CN (3:1), the characteristic signals of the Cl^--bound crosslinks could be observed after an equilibration time of 12 hours (see the Supporting Information, Figure S38). These findings suggested that chloride ions could trigger the release of abiraterone from **NGel 2**.

To quantitatively assess drug release, purified **NGel 2** was dispersed into a dialysis device and dialyzed against a mixture of H_2O and acetone (1:1) for 12 hours at room temperature. Subsequently, the dialysate was concentrated and analyzed by ^1H NMR using dimethyl terephthalate as an internal standard. The ^1H NMR spectrum confirmed that the drug was not released in the absence of NaCl (Figure S40). Subsequently, **NGel 2** was mixed with NaCl (1.1 equivalent relative to the theoretical crosslink concentration) in H_2O and equilibrated for 12 hours. The dispersion was then placed again in a dialysis device and the release of abiraterone was monitored (Figure 4). After a dialysis time of 24 hours, more than 25 % of the abiraterone in **NGel 2** was released. These findings underscore the potential utility of the nanogel as a platform for controlled, chloride-induced drug release.

Conclusions

To date, there is limited literature regarding the utilization of coordination complexes as responsive constituents in micro or nanogels. We have demonstrated that metal-organic cages can serve as functional crosslinks in NIPAM-based nanogels. Two distinct gels were synthesized, each incorporating structurally related metal-ligand assemblies. In **NGel 1**, homoleptic Pd_2L_4 complexes were utilized as crosslinks. The original host properties of the cages remained intact within the gel matrix, enabling the nanogel to function as a proficient sorbent for chloride ions in aqueous solution. The second nanogel, **NGel 2**, was obtained by co-polymerization of NIPAM with a heteroleptic cage, featuring the anticancer drug abiraterone as a co-ligand. Chloride ions induced a structural rearrangement of the metal-ligand assembly, resulting in the gradual release of

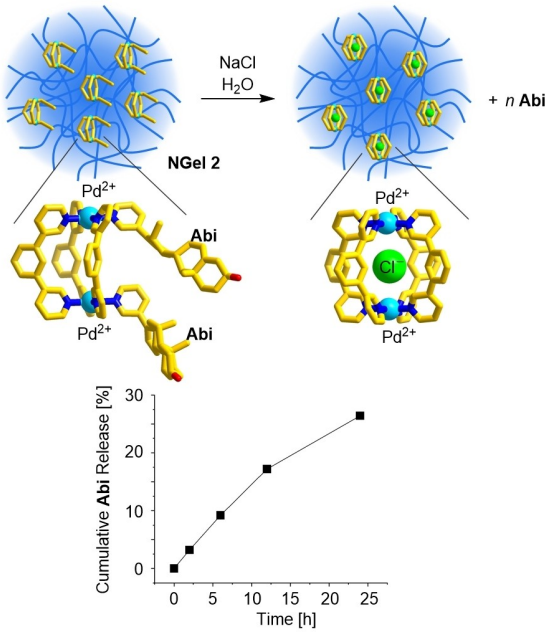

Figure 4. Chloride-induced release of **Abi** from **NGel 2** as determined by NMR spectroscopy after different dialysis times.

abiraterone. Overall, our findings represent evidence that metal-organic cages can be employed to prepare nanogels with unique functions and properties.

Acknowledgements

We acknowledge support from the Ecole Polytechnique Fédérale de Lausanne (EPFL). We thank Dr. Davide Demurtas (EPFL) and Dr. David Reyes (EPFL) for the TEM measurements and analyses, and Sylvain Sudan for providing ligand **L2** and for his valuable suggestions. Open Access funding provided by École Polytechnique Fédérale de Lausanne.

Conflict of Interest

The authors declare no conflict of interest.

Data Availability Statement

The data that support the findings of this study are available in the supplementary material of this article.

Keywords: anion receptor · cage · coordination compound · nanogel · metallosupramolecular chemistry

[1] For general reviews, see: a) X. Xu, H. Zhu, A. Denduluri, Y. Ou, N. A. Erkamp, R. Qi, Y. Shen, T. P. J. Knowles, *Small* **2020**, *18*, 2200180; b) M. Karg, A. Pich, T. Hellweg, T. Hoare, L. A. Lyon, J. J. Crassous, D. Suzuki, R. A. Gumerov, S. Schneider, I. I. Potemkin, W. Richtering, *Langmuir* **2019**, *35*, 6231–6255; c) R. Begum, Z. H. Farooqi, E. Ahmed, A. Sharif, W. Wu, A. Irfan, *RSC Adv.* **2019**, *9*, 13838; d) F. A. Plamper, W. Richtering, *Acc. Chem. Res.* **2017**, *50*, 131–140; e) S. Nayak, L. A. Lyon, *Angew. Chem. Int. Ed.* **2005**, *44*, 7686–7708; f) B. R. Saunders, B. Vincent, *Adv. Colloid Interface Sci.* **1999**, *80*, 1–25.

[2] a) G. Agrawal, R. Agrawal, *Polymer* **2018**, *10*, 418; b) D. Klinger, K. Landfester, *Polymer* **2012**, *53*, 5209–5231.

[3] a) G. Agrawal, R. Agrawal, *Small* **2018**, *14*, 1801724; b) Z. Dai, T. Ngai, *J. Polym. Sci. Part A* **2013**, *51*, 2995–3003; c) Y. Guan, Y. Zhang, *Soft Matter* **2011**, *7*, 6375–6384; d) H. Bysell, R. Månsson, P. Hansson, M. Malmsten, *Adv. Drug Delivery Rev.* **2011**, *63*, 1172–1185; e) J. K. Oh, R. Drumright, D. J. Siegwart, K. Matyjaszewski, *Prog. Polym. Sci.* **2008**, *33*, 448–477.

[4] a) M. Karg, *Colloid Polym. Sci.* **2012**, *290*, 673–688; b) J. B. Thorne, G. J. Vin, M. J. Snowden, *Colloid Polym. Sci.* **2011**, *289*, 625–646.

[5] a) M. Shahid, Z. H. Farooqi, R. Begum, M. Arif, W. Wu, A. Irfan, *Crit. Rev. Anal. Chem.* **2020**, *50*, 513–537; b) Z. H. Farooqi, S. R. Khan, R. Begum, *Mater. Sci. Technol.* **2017**, *33*, 129–137; c) R. Begum, K. Naseem, Z. H. Farooqi, *J. Sol-Gel Sci. Technol.* **2016**, *77*, 497–515; d) N. Welsch, M. Ballauff, Y. Lu, *Adv. Polym. Sci.* **2010**, *234*, 129–163.

[6] L. A. Lyon, Z. Meng, N. Singh, C. D. Sorrell, A. St. John, *Chem. Soc. Rev.* **2009**, *38*, 865–874.

[7] a) A. Brézault, P. Perrin, N. Sanson, *Macromolecules* **2024**, *57*, 2651–2660; b) J. E. Sayed, C. Meyer, N. Sanson, P. Perrin, *ACS Macro Lett.* **2020**, *9*, 1040–1045.

[8] a) J. E. Sayed, C. Lorthioir, P. Banet, P. Perrin, N. Sanson, *Angew. Chem. Int. Ed.* **2020**, *59*, 7042–7048; b) J. Lee, E. J. Choi, I. Varga, P. M. Claesson, S.-H. Yun, C. Song, *Polym. Chem.* **2018**, *9*, 1032–1039; c) M. Gerth, M. Bohdan, R. Fokkink, I. K. Voets, J. Van der Gucht, J. Sprakel, *Macromol. Rapid Commun.* **2014**, *35*, 2065–2070.

[9] a) T. Tateishi, M. Yoshimura, S. Tokuda, F. Matsuda, D. Fujita, S. Furukawa, *Coord. Chem. Rev.* **2022**, *467*, 214612; b) A. J. McConnell, *Chem. Soc. Rev.* **2022**, *51*, 2957–2971; c) A. V. Virovets, E. Peresypkina, M. Scheer, *Chem. Rev.* **2021**, *121*, 14485–14554; d) S. Pullen, J. Tessarolo, G. H. Clever, *Chem. Sci.* **2021**, *12*, 7269–7293; e) G. E. Decker, G. R. Lorzing, M. M. Deegan, E. D. Bloch, *J. Mater. Chem. A* **2020**, *8*, 4217–4229.

[10] a) E. G. Percástegui, *Chem. Commun.* **2022**, *58*, 5055–5071; b) D. Zhang, T. K. Ronson, Y.-Q. Zou, J. R. Nitschke, *Nat. Chem. Rev.* **2021**, *5*, 168–182; c) E. J. Gosselin, C. A. Rowland, E. D. Bloch, *Chem. Rev.* **2020**, *120*, 8987–9014; d) F. J. Rizzuto, L. K. S. von Krebek, J. R. Nitschke, *Nat. Chem. Rev.* **2019**, *3*, 204–222.

[11] a) T. K. Piskorz, V. Mart-Centelles, R. L. Spoicer, F. Duarte, P. J. Lusby, *Chem. Sci.* **2023**, *14*, 11300; b) M. Otte, *Eur. J. Org. Chem.* **2023**, *26*, e202300012; c) R. Ham, C. J. Nielsen, S. Pullen, J. N. H. Reek, *Chem. Rev.* **2023**, *123*, 5225–5261; d) R. Saha, B. Mondal, P. S. Mukherjee, *Chem. Rev.* **2022**, *122*, 12244–12307; e) P. Howlander, M. Schmittel, *Beilstein J. Org. Chem.* **2022**, *18*, 597–630; f) Y. Xue, X. Hang, J. Ding, B. Li, R. Zhu, H. Pang, Q. Xu, *Coord. Chem. Rev.* **2021**, *430*, 213656; g) A. B. Grommet, M. Feller, R. Klajn, *Nat. Nanotechnol.* **2020**, *15*, 256–271; h) A. C. H. Jans, X. Caumes, J. N. H. Reek, *ChemCatChem* **2019**, *11*, 287–297.

[12] a) E. Benchimol, J. Tessarolo, G. H. Clever, *Nat. Chem.* **2024**, *16*, 13–21; b) H.-Y. Lin, Y.-T. Wang, X. Shi, H.-B. Yang, L. Xu, *Chem. Soc. Rev.* **2023**, *52*, 1129–1154; c) E. Benchimol, B.-N. T. Nguyen, T. K. Ronson, J. R. Nitschke, *Chem. Soc. Rev.* **2022**, *51*, 5101–5135; d) A. Díaz-Moscoso, P. Ballester, *Chem. Commun.* **2017**, *53*, 4635–4652.

[13] a) W. Drożdż, A. Ciesielski, A. R. Stefankiewicz, *Angew. Chem. Int. Ed.* **2023**, *62*, e202307552; b) P. Liu, F. Fang, H. Wang, N. M. Khashab, *Angew. Chem. Int. Ed.* **2023**, *62*, e202218706; c) E. Sánchez-González, M. Y. Tsang, J. Troyano, G. A. Craig, S. Furukawa, *Chem. Soc. Rev.* **2022**, *51*, 4876–4889; d) I. Jahović, Y.-Q. Zou, S. Adorinni, J. R. Nitschke, S. Marchesan, *Matter* **2021**, *4*, 2123–2140; e) Y. Zhu, W. Zheng, W. Wang, H.-B. Yang, *Chem. Soc. Rev.* **2021**, *50*, 7395–7417; f) V. J. Pastore, T. R. Cook, *Chem. Mater.* **2020**, *32*, 3680–3700; g) Y. Gu, J. Zhao, J. A. Johnson, *Angew. Chem. Int. Ed.* **2020**, *59*, 5022–5049; h) K. C. Bentz, S. M. Cohen, *Angew. Chem. Int. Ed.* **2018**, *57*, 14992–15001.

[14] R.-J. Li, F. Fadaei-Tirani, R. Scopelliti, K. Severin, *Chem. Eur. J.* **2021**, *27*, 9439–9445.

[15] S. Sudan, D. W. Chen, C. Berton, F. Fadaei-Tirani, K. Severin, *Angew. Chem. Int. Ed.* **2023**, *62*, e202218072.

[16] a) N. Sanson, J. Rieger, *Polym. Chem.* **2010**, *1*, 965–977; b) A. Pich, W. Richtering, *Adv. Polym. Sci.* **2010**, *234*, 1–37.

[17] As detailed in ref. 15, the cage binds in aqueous solution bromide along with chloride, but not fluoride, sulfate, acetate, carbonate, or phosphate. A similar selectivity is expected for **NGel 1**.

[18] M. N. Stein, S. Goodin, R. S. DiPaola, *Clin. Cancer Res.* **2012**, *18*, 1848–1854.

Manuscript received: February 23, 2024
Accepted manuscript online: April 5, 2024
Version of record online: ■■, ■■

Research Articles

Polymer Chemistry

C. Hu, K. Severin* _____ e202403834

Nanogels with Metal-Organic Cages as Functional Crosslinks

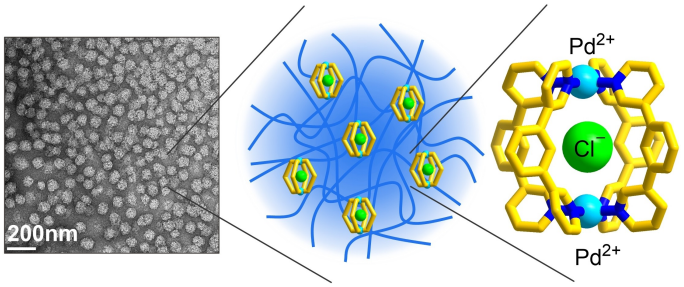

Palladium-organic cages with acrylamide side chains were incorporated in N-isopropylacrylamide-based nanogels by precipitation polymerization. Due to the presence of cage crosslinks, the resulting nanogels can be used as specific sorbents for chloride ions.